Reliability Characterization of Tantalum Capacitors with MnO_2 Counter-Electrode

Jonathan L. Paulsen
KEMET Electronics Corp.
PO Box 5928, Greenville, SC 29606
1-864-963-6300 (Phone) / 1-864-967-6876 (FAX)
jonathanpaulsen@kemet.com (EMAIL)

Abstract

Reliability analysis of capacitors manufactured with manganese dioxide (MnO_2) solid electrolyte has traditionally been accomplished using Weibull failure rate grading. This method was developed decades ago using time-to-failure data from many tantalum capacitor samples with varying manufacturers and production specifications. Subsequent investigations have demonstrated that factors affecting reliability analysis can vary substantially for different MnO_2 capacitor designs. Since traditional Weibull characterization assumes similar performance for all parts regardless of process parameters, more refined reliability experiments may yield more useful information.

The aim of this work is to develop a more flexible framework for reliability analysis of MnO_2 tantalums. To achieve this goal within a reasonable timeframe, accelerated lifetesting utilizing high electric field stress and temperature was performed on multiple test samples. The resulting time-to-failure data was fit to a failure model and then used to predict device reliability under less strenuous conditions.

Introduction

Over the last several years, the accelerated lifetesting methodology described in this paper, originally proposed by Procopowicz and Vaskas[1], has been utilized to examine the reliability of both base metal electrode ceramic and polymer tantalum capacitors. For base metal ceramics, the goal of the experiment was to determine the impact of a known wearout mechanism on lifetest performance[3]. For polymer tantalums, their reliability was under scrutiny due to their recent commercial availability at the time.

The experiments on these parts produced well organized time-to-failure data that identified wearout mechanisms in these devices. Further, the results suggested the test strategy was capable of predicting usable lifetimes for the parts at conditions other than those used in the experiments [2, 4].

To compliment the previous work, applying this reliability analysis to tantalum capacitors made with a more traditional MnO_2 counter electrode seemed a logical next step. Accelerated lifetest analysis of MnO_2 tantalums has traditionally been accomplished using Weibull failure rate grading as outlined in military performance specification 39003J. The capacitors were exposed to a multiple of rated voltage, typically 1.1 to 1.5 times rated voltage, and tested at 85°C until a sufficient number of failures were observed for calculations. The acceleration

of time-to-failure for each test batch was obtained using equation (1).

$$A = 7.03412025 \times 10^{-9} e^{18.77249321 \times \frac{V_a}{V_r}} \quad (1)$$

Since investigations have demonstrated that acceleration factor can vary widely from batch to batch among similar devices, this equation did not apply particularly well to any traditional tantalum part type. Additionally, the time-to-failure results of Weibull testing are often quite sparse and offer little insight into the reliability of the devices.

In the present experiment, 10µF, 16V tantalum capacitors made with MnO2 counter electrodes and packaged in an EIA 3062-28 case were lifetested with enough temperature and voltage acceleration to actually reach wearout within a reasonable timeframe.

Failure Modeling

An established formula for modeling acceleration in time for capacitor lifetest failures as a function of voltage and temperature is the equation proposed by Prokopowicz and Vaskas, shown in equation (2).[1]

$$\frac{t_1}{t_2} = \left(\frac{V_2}{V_1}\right)^{\eta} e^{\left[\frac{Ea}{k}\left(\frac{1}{T_1} - \frac{1}{T_2}\right)\right]} \quad (2)$$

The formula relates the ratio of different times-to-failure to the applied voltage and ambient temperature of two different test conditions. The formula can be broken into two parts. The power law portion of equation (2) quantifies time-to-failure acceleration due to the ratio of two voltages. The voltage stress exponent in the power law equation, n, must be experimentally derived. The second half of equation (2) accounts for time-to-failure acceleration due to changes in absolute temperature. This portion of the relation is modeled by an Arrhenius equation. The activation energy in the Arrhenius equation, Ea, must also be derived experimentally before equation (2) can be used.

The constant, k, is Boltzmann's constant. The approximate value for k is shown in equation (3). Absolute temperature in Kelvins is the temperature in Celsius degrees plus 273.

$$k = 8.6 \times 10^{-5}\, eV / K \quad (3)$$

The time-to-failure data produced in this experiment was plotted on lognormal graphs rather than Weibull plots. Previously, time-to-failure data for tantalum capacitors was generally fit to a Weibull distribution for analysis. For Weibull plots, the statistic $t_{63.2}$, or characteristic life, is chosen rather than the median life, t_{50}. The time-to-failure data collected in this experiment was initially fit to both Weibull and lognormal distributions. The lognormal distribution provided superior fit to the data. As a result, the median life statistic, t_{50}, was used to calculate the voltage stress exponent as well as the activation energy for use in equation (2).

System Description

The block diagram for the time-to-failure system used for these experiments is shown in figure 1.

This test system comprises seven basic elements. The test parts are mounted onto test cards which are placed into connectors mounted to a fixture within the test chamber. The test card fixture has multiple 22 position connectors rated for use at high temperatures (up to 200°C). The number of connectors within the system depends upon the size of the test chamber and the desired sample size for the test. Fixtures used for these experiments range from 5 to 12 connectors. The test chamber itself is a general purpose environmental chamber capable of operation at temperatures from -55°C to 250°C. Wires soldered to the high-temp connectors are routed through a port in the test chamber to a rack outside the test environment which holds 1 amp fuses connected in series with each part under test. Each test part circuit has a resistance below 600mΩ. The entire fuse rack is wired to the output of a DC power supply. A 10mΩ current measurement resistor is placed in series with the negative power supply lead. A high speed digital voltmeter is connected across the 10mΩ resistor to measure any voltage caused by current passing through the test system. The voltmeter communicates with a computer running software which detects failures as they occur and records their time relative to the start of the test. Furthmore, the resistance of each card in the fuse rack is checked before testing. The maximum allowable resistance for each position in the fuse card is 200mΩ.

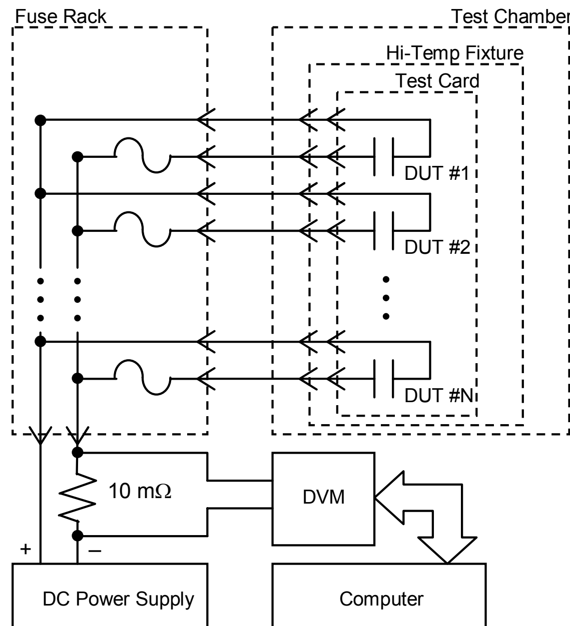

Fig. 1. Time-To-Failure System Block Diagram.

Analysis of KEMET MnO_2 Tantalum Time-To-Failure Data

Figure 1 is a crowded graph that contains all of the time-to-failure data collected from a batch of KEMET 10uF, 16V MnO_2 tantalum capacitors. The same data will also be shown in subsets, but all the data presented at once enables important observations.

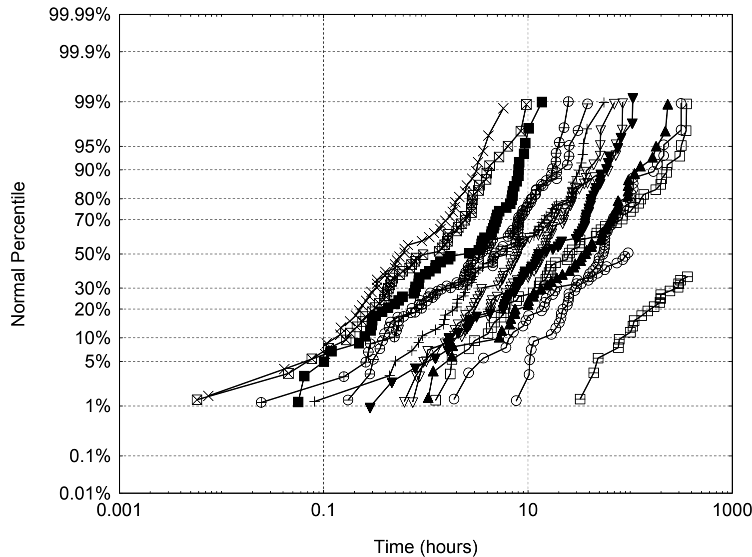

Fig. 2. Lognormal Plot of Failure Percentile versus Time-to-Failure for KEMET MnO2 Ta Caps.

The test conditions included four temperatures (85°C, 125°C, 140°C, and 165°C) and eight voltages (28.8V, 32.0V, 35.2V, 36.8V, 38.4V, 41.6V, 44.8V, and 48.0V). Median life under the various test conditions ranged over almost two orders of magnitude (1 hour to nearly 100 hours).

Three failure mechanisms are of interest when lifetesting electronic devices: Infant mortals, freaks, and wearout failures. Infant mortals contain major construction defects and never function properly. Freak failures have minor construction defects that will eventually cause failure, but perhaps years after initial usage. Wearout failures, the focus of this experiment, only occur after the dielectric within the capacitor changes due to applied electric field stress. Accelerated testing is a good method to diagnose all three of these mechanisms. On a time-to-failure graph, each failure mechanism will appear as a subpopulation requiring a different "best fit" line. Some of the early failures on the graphs shown may be attributable to freak failures, their presence causing a slight curve at the bottom of the distribution. Despite interest in these failures, they have been ignored in this discussion of wearout, and not used in the statistical calculations. The relatively straight lines on the graph suggest that the majority of the failures were caused by one failure mechanism. Given the severity of accelerated testing, it is important to note that no new failure mechanisms were introduced.

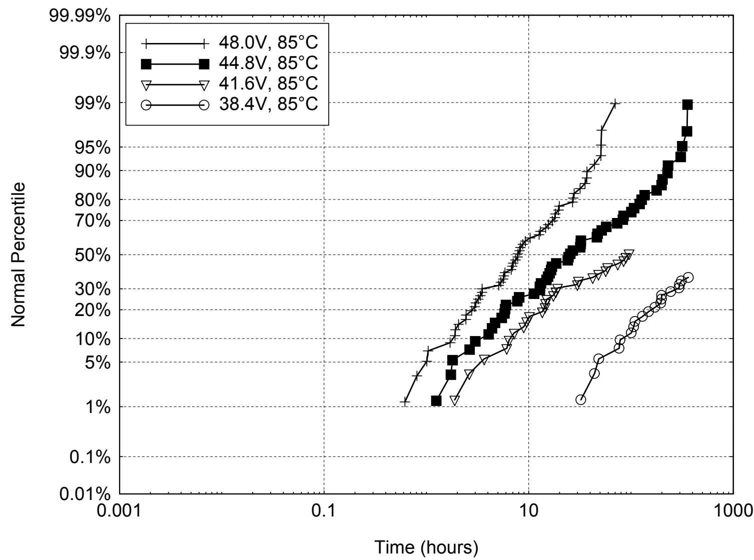

Fig. 3. Lognormal Plot of Failure Percentile versus Time-to-Fail at 48.0V, 44.8V, 41.6V, and 38.4V for tests done at 85°C.

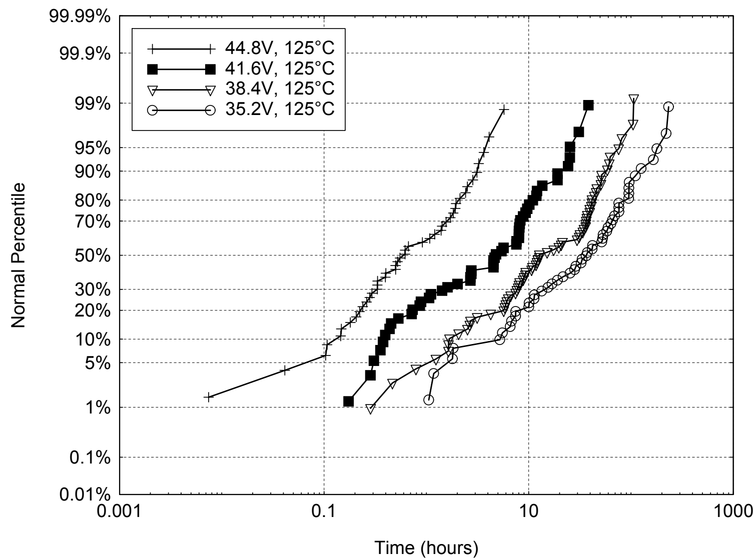

Fig. 4. Lognormal Plot of Failure Percentile versus Time-to-Fail at 44.8V, 41.6V, 38.4V and 35.2V for Tests at 125°C.

Data collected at 85°C and four voltages appear in Figure 3. The failure distributions are similar and the spacing is reasonably uniform as the voltage stress is increased. The partial results 41.6V and 38.4V were due to an accidental test interruption before their completion.

Figures 4, 5 and 6 contain the data collected at 125°C, 140°C and 165°C, respectively. Again, as the voltage is decreased, the spacing and slope of the failure curves remains reasonably uniform.

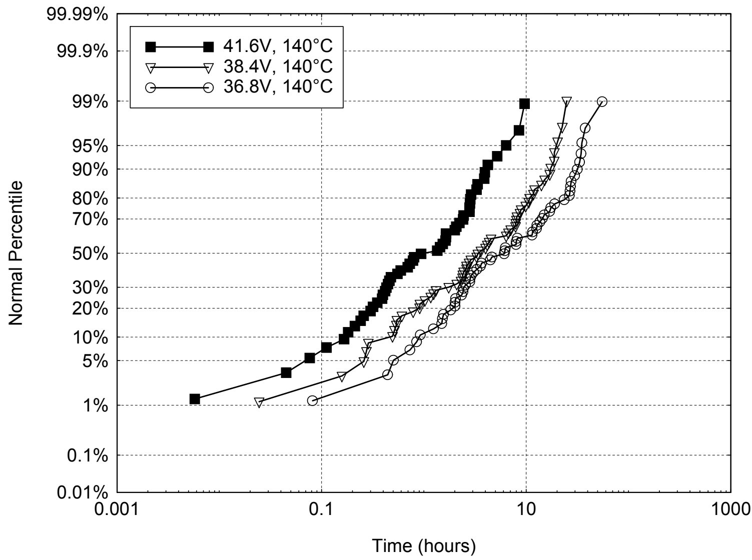

Fig. 5. Lognormal Plot of Failure Percentile versus Time-to-Failure at 41.6V, 38.4V, and 36.8V for Tests Done at 140°C.

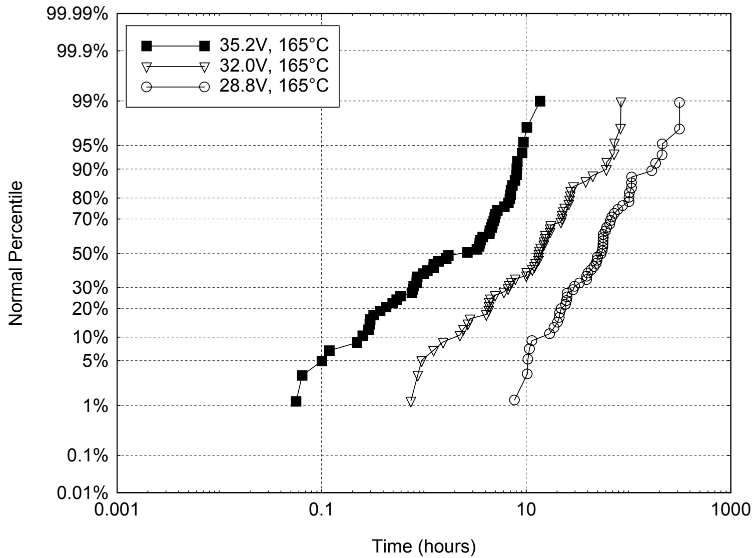

Fig. 6. Lognormal Plot of Failure Percentile versus Time-to-Failure at 35.2V, 32.0V, and 28.8V for Tests Done at 165°C.

Figure 7 is a plot of median life, t_{50}, versus test voltage at 85°C, 125°C, 140°C and 165°C. In this figure, each failure distribution discussed above is expressed as a single statistic, t_{50}, and is plotted on a "log-log" scale. Four lines were fit to the data points and the equations of the lines appear in the legend. The exponents for these straight lines range from n=16 at 165°C to n=18.5 at 85°C. It is not known whether the range of values observed for the voltage acceleration exponent reflects temperature dependence of voltage acceleration, experimental error, or some combination of both.

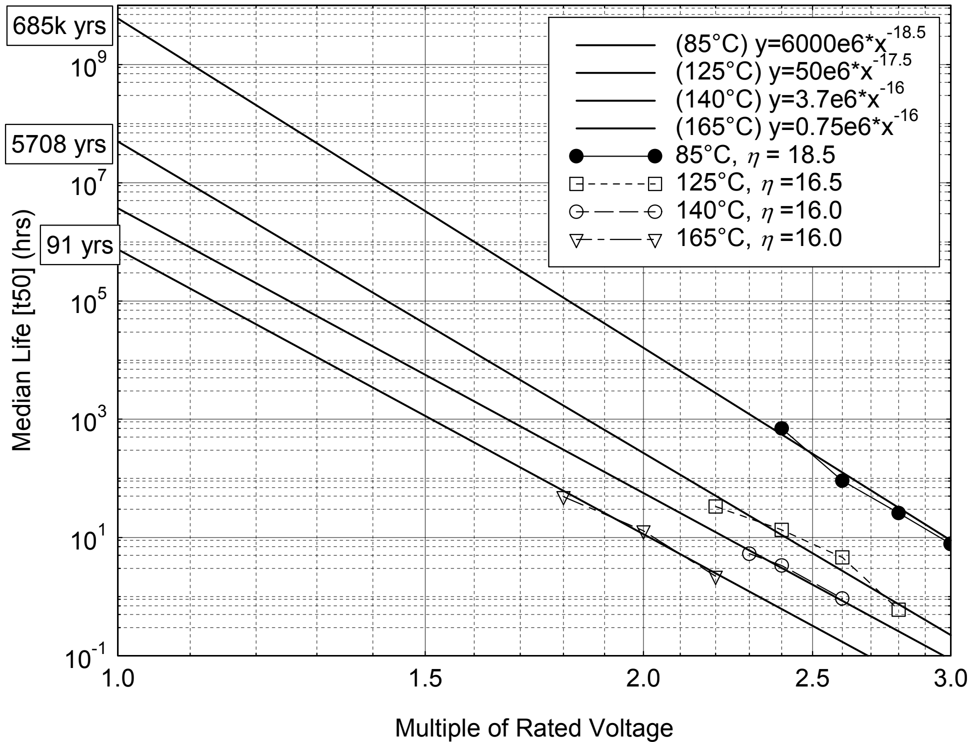

Fig. 7. Plot of Median Life versus Test Voltage at 85°C, 125°C, 140°C and 165°C on Log-Log Scale.

The x-axis of figure 7 extends down to rated voltage. This enables an estimate of life test performance at the maximum rated conditions for the parts. Following the line of 85°C results back to the rated voltage point, the fit line indicates these parts would reach their t_{50} after several hundred thousand years at maximum rated conditions. Note how reasonably uniform the slopes of the best fit lines appear. It is worth noting that there seems to be less interaction between voltage and temperature than was observed during accelerated testing of polymer tantalums[4, 2]. This interaction manifested itself by altering the slope of the fit lines dramatically as temperature stress increased.

The preceding discussion has been focused on voltage acceleration. The next set of graphs will highlight the effect of temperature acceleration. The same time-to-failure data will be analyzed, but the failure curves will be grouped by voltage rather than by temperature.

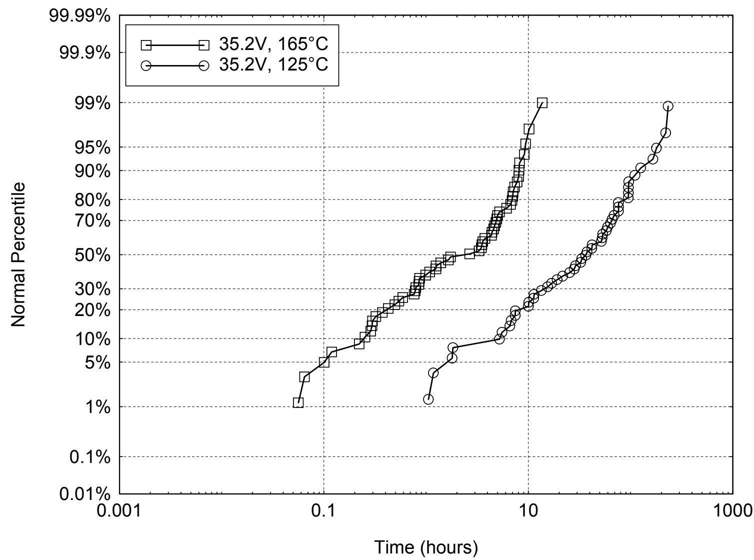

Fig. 8. Lognormal Plot of Failure Percentile versus Time-to-Failure at 125°C and 165°C for Tests Done at 35.2V.

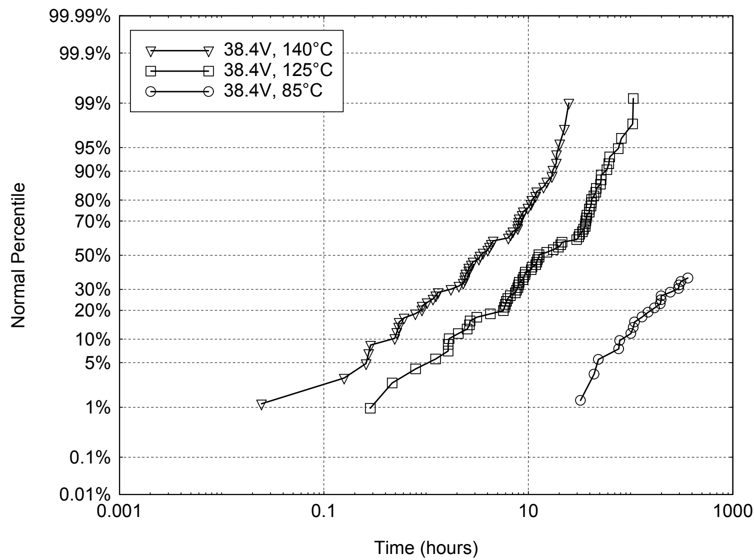

Fig. 9. Lognormal Plot of Failure Percentile versus Time-to-Failure at 85°C, 125°C, and 140°C for Tests Done at 38.4V.

Data collected at 35.2V, 38.4V, 41.6V, 44.8V and 48.0V and several temperatures appear in Figures 8-11. Again, the failure distributions are similar and that the spacing is reasonably uniform as the temperature is changed from 85°C to 165°C.

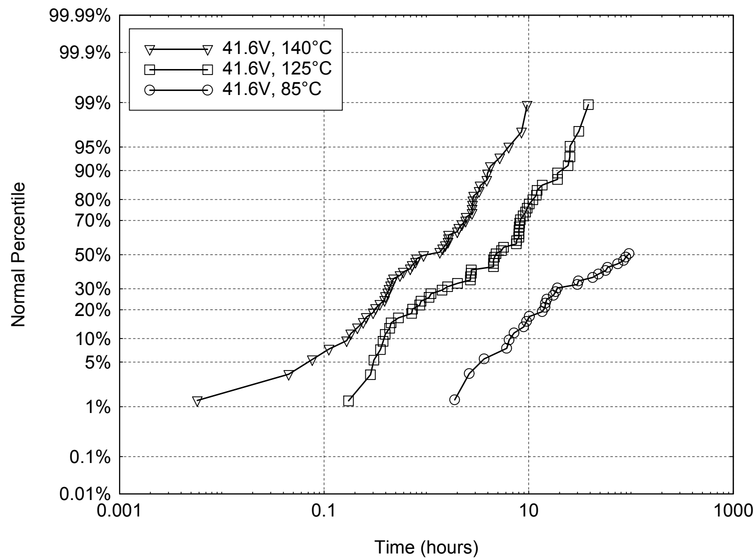

Fig. 10. Lognormal Plot of Failure Percentile versus Time-to-Failure at 85°C, 125°C and 140°C for Tests Done at 41.6V.

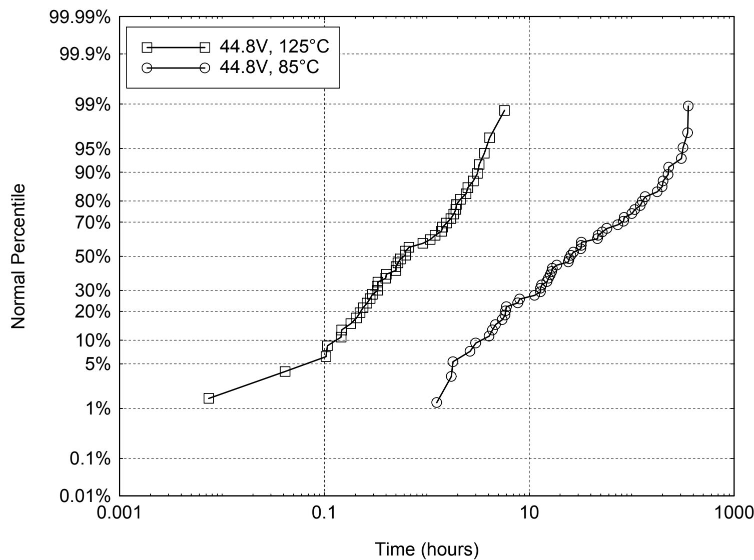

Fig. 11. Lognormal Plot of Failure Percentile versus Time-to-Failure at 85°C and 125°C for Tests Done at 44.8V.

Figure 12 is a plot of median life, t_{50}, versus inverse absolute temperature at 2.2Vr, 2.4Vr, 2.6Vr and 2.8Vr. In this figure, each failure distribution is represented by its t_{50}, and is plotted on a "semi-log" scale to form straight lines with the data.

Once fit lines have been placed over the data points, the activation energies for the test groups emerge as values ranging from 1.08eV to 1.15eV. These values are lower than those observed during polymer tantalum testing[2].

As in Figure 7, it is possible to observe the impact of voltage on median life in Figure 12. The spacing between the lines which were fit to the data collected at 2.2Vr, 2.4Vr, 2.6Vr and 2.8Vr is reasonably uniform. So, it seems logical to continue this spacing to see what performance is projected at 16V. A line is included in the figure that is consistent with the known failure data and E_a=1.15. This line projects a median life in excess of 7000 years at 16V and 85°C.

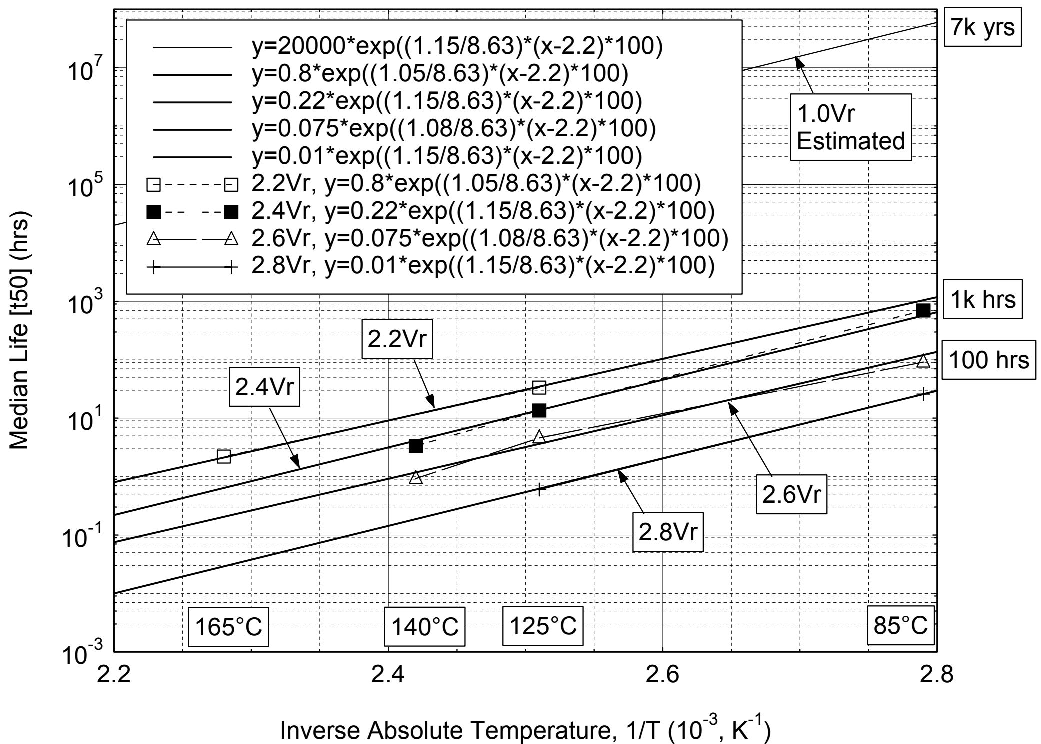

Fig. 12. Plot of Median Life versus Inverse Absolute Temperature at 2.2Vr, 2.4Vr, 2.6Vr and 2.8V.

Clearly, a substantial gap exists between the projected line at 16V and the lines that represent testing at higher voltages. Unfortunately, there is no practical way to avoid the uncertainty inherent to such a prediction. However, the projected life at maximum rated conditions is far in excess of that needed for even the most demanding tantalum capacitor applications.

SUMMARY AND CONCLUSIONS

It has been shown through these experiments that time-to-failure distributions of MnO_2 tantalum chip capacitors do not significantly alter their shape even when the applied stress is

significantly accelerated during testing. Therefore, it is likely that no new failure mechanisms are introduced under these highly accelerated conditions.

Plots of median life versus test voltage and temperature produce families of curves that are proportionately spaced and reasonably linear when appropriately scaled with respect to Prokopowicz and Vaskas acceleration model. Thus, one concludes that time-to-failure under more normal conditions (at or below maximum device ratings) can be projected with reasonable confidence by applying Prokopowicz' model and values of n and E_a that are derived from accelerated testing of sample populations of those devices.

For the devices tested in this study, projected median life at maximum rated conditions was more than several thousand years. These results correlate with the already well-established reliability record of properly constructed MnO_2 tantalums while operating in well-designed applications.

REFERENCES

[1] T. Prokopowicz and A. Vaskas, "Research and Development, Intrinsic Reliability, Subminiature Ceramic Capacitors," Final Report, ECOM-90705-F, 1969 NTIS AD-864068.

2 J. Paulsen, E. Reed, and J. Kelly, "Reliability of Tantalum Polymer Capacitors," CARTS '04 Proceedings of the 24th Capacitor and Resistor symposium, (2004).

3 J. Paulsen and E. Reed, "Highly Accelerated Lifetesting (HALT) of KEMET Base-Metal-Electrode (BME) Ceramic Chip Capacitors," CARTS '01 Proceedings of the 21st CARTS (2001).

4 E. Reed, J. Kelly and J. Paulsen, "Reliability of Low-Voltage Tantalum Polymer Capacitors," CARTS '05 Proceedings of the 25th CARTS (2005).